AGU PUBLICATIONS

Journal of Advances in Modeling Earth Systems

RESEARCH ARTICLE
10.1002/2013MS000268

Key Points:
- CAM-SE conserves global axial angular momentum (AAM) well
- Vertical coordinate/polynomial order does not impact AAM properties
- CAM-SE dynamical core is well suited for Venus/Titan simulations

Correspondence to:
P. H. Lauritzen,
pel@ucar.edu

Citation:
Lauritzen, P. H., J. T. Bacmeister, T. Dubos, S. Lebonnois, M. A. Taylor (2014) Held-Suarez simulations with the Community Atmosphere Model Spectral Element (CAM-SE) dynamical core: A global axial angular momentum analysis using Eulerian and floating Lagrangian vertical coordinates *J. Adv. Model. Earth Syst. 6*, 129–140, doi:10.1002/2013MS000268

Received 16 SEP 2013
Accepted 21 JAN 2014
Accepted article online 28 JAN 2014
Published online 24 FEB 2014

Held-Suarez simulations with the Community Atmosphere Model Spectral Element (CAM-SE) dynamical core: A global axial angular momentum analysis using Eulerian and floating Lagrangian vertical coordinates

Peter H. Lauritzen[1], Julio T. Bacmeister[1], Thomas Dubos[2], Sébastien Lebonnois[3,4], and Mark A. Taylor[5]

[1]Climate and Global Dynamics Division, National Center for Atmospheric Research, Earth System Laboratory, Boulder, Colorado, USA, [2]Ecole Polytechnique, UMR 8539, Laboratoire de Météorologie Dynamique/IPSL, Palaiseau, France, [3]Sorbonne Universités, UPMC Univ Paris 06, UMR 8539, Laboratoire de Météorologie Dynamique/IPSL, Paris, France, [4]Centre National de la Recherche Scientifique, UMR 8539, Laboratoire de Météorologie Dynamique/IPSL, Paris, France, [5]Sandia National Laboratories, Albuquerque, New Mexico, USA

Abstract In this paper, an analysis of the global AAM conservation properties of NCAR's Community Atmosphere Model Spectral Element (CAM-SE) dynamical core under Held-Suarez forcing is presented. It is shown that the spurious sources/sinks of AAM in CAM-SE are 3 orders of magnitude smaller than the parameterized (physical) sources/sinks. The effect on AAM conservation by changing various numerical aspects of the dynamical core (e.g., different vertical coordinates, reduced formal order of accuracy, increased dissipation, and decreased divergence damping) is investigated. In particular, it is noted that changing from Eulerian (hybrid-sigma) to floating Lagrangian vertical coordinates does not alter the global AAM conservation properties of CAM-SE.

1. Introduction

The angular momentum of an atmosphere with respect to its rotation axis characterizes its rotary inertia and it is a fundamental physical quantity characterizing the general circulation. In the absence of any surface torque and zonal mechanical forcing, the hydrostatic primitive equations conserve the globally integrated axial angular momentum (AAM) [*Thuburn*, 2008] when assuming a constant pressure upper boundary condition [see, e.g., *Staniforth and Wood*, 2003]. The fluid flow solver (also known as the dynamical core) approximating the solution to the hydrostatic primitive equations should therefore ideally also conserve AAM, however, no dynamical core known to the authors conserves AAM to machine precision. For axisymmetric flows, *Hourdin* [1992] derived a vertical discretization that compensates for the lack of AAM in the horizontal discretization. Hyperviscosity operators can be formulated so that uniform rotation is not affected and thereby the operator is not a source/sink for AAM for that part of the flow (see, e.g., Section 3.3.6 in *Neale et al*. [2010]).

Accurate conservation of AAM in the dynamical core has been found particularly important for modeling superrotating atmospheres such as the atmospheres of Venus and Titan [e.g., *Lebonnois et al*., 2012, hereafter Leb2012]. If the spurious sources/sinks of AAM in the dynamical core are of similar or larger magnitude than the physical torques, the credibility of the simulation is dubious. Leb2012 found that this was the case in Venus/Titan simulations as well as simplified Earth simulations (see Figure 1) when using NCAR's CAM (Community Atmosphere Model) [*Neale et al*., 2010] adapted for the Venus atmosphere and using the finite-volume dynamical core (referred to as CAM-FV) [*Lin*, 2004]. Similarly, *Lee and Richardson* [2010] found that the simulation of the general circulation of Venus's atmosphere varied significantly between different dynamical cores (the "B-core" (http://math.nyu.edu/∼gerber/pages/climod/bgrid.pdf), a spectral transform dynamical core [*Held and Suarez*, 1994], and a finite-volume (FV) dynamical core [*Lin*, 2004] available in the Geophysical Fluid Dynamics Laboratory (GFDL) Flexible Modeling System (FMS)). In particular, it was noted that the damping operators were very different between the dynamical cores. The superior performing model, in terms of credible atmospheric state, conserved AAM very well [*Lee and Richardson*, 2012].

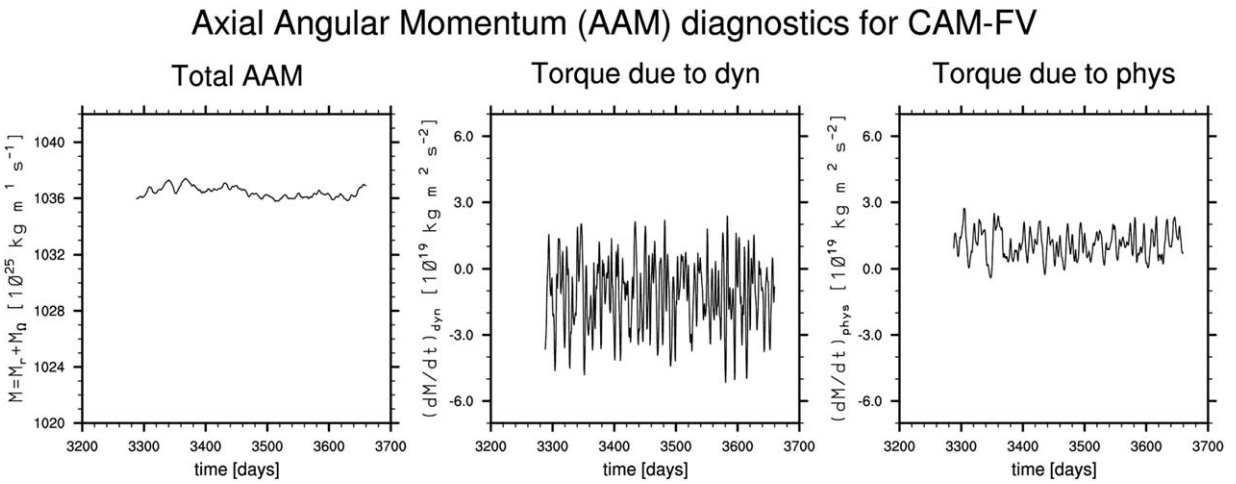

Figure 1. Angular momentum diagnostics for CAM-FV in the Held-Suarez setup (data are from *Lebonnois et al*. [2012]). First, second, and third column is total angular momentum (M_r+M_Ω), time tendencies of AAM due to the dynamical core $\left(\left(\frac{dM}{dt}\right)_{dyn}\right)$ and physical parameterizations $\left(\left(\frac{dM}{dt}\right)_{phys}\right)$, respectively, as a function of time. Note that the spurious source/sinks of AAM from the dynamical core (second column) are the same order of magnitude as the physical sources/sinks of AAM (third column).

In Earth's atmosphere, the physical sources/sinks of angular momentum are very large. On the resolved scales (part of the dynamical core), there are large mountain torques due to pressure difference across orography. The mountain torques are predominantly eastward in the tropics and westward in the midlatitudes, and this AAM exchange affects the length of day [see, e.g., *Egger et al*., 2007]. On the unresolved scales, the frictional forces such as boundary layer turbulence and drags from breaking gravity waves alter the AAM budget. Due to these large physical sources and sinks (that are not in a similar balance as for Venus and Titan), the lack of conservation of AAM in the dynamical core (when subtracting the mountain torque) is much less apparent.

It is the purpose of this paper to investigate the globally integrated AAM conservation properties of the spectral-element dynamical core (the CAM-SE dynamical core is the continuous Galerkin spectral finite-element dynamical core in NCAR's High-Order Method Modeling Environment (HOMME) [*Dennis et al*., 2005]; referred to as CAM-SE [*Dennis et al*., 2012]) and to investigate how different numerical operators/options available in CAM-SE affect AAM conservation. The CAM-SE dynamical core can be run at different formal orders of accuracy (by varying the order of the polynomial basis functions) and it accommodates two different treatments of vertical advection that are commonly used: the finite difference treatment of vertical advection that conserves angular momentum and total energy [*Simmons and Burridge*, 1981], which will be referred to as *Eulerian* vertical coordinate (hybrid-sigma), and the floating Lagrangian vertical coordinates for which the vertical advection terms are essentially replaced by periodic vertical remapping of prognostic variables from the floating Lagrangian layers to reference Eulerian (hybrid-sigma) vertical coordinates. This remapping also conserves AAM and optionally total energy [*Lin*, 2004]. The effect on AAM conservation by using these different numerical operators is the main topic of this paper. The AAM analysis is detailed in the sense that not only are the total contributions to AAM from the dynamical core and parameterizations separated but also the breakdown into the relative contributions from diffusion operators and the "inviscid" fluid flow solver. The AAM diagnostics are computed consistently inline in the dynamical core at every dynamics time step and fully consistently with the spectral-element method.

The simulations presented here make use of the idealized Earth configuration called Held-Suarez [*Held and Suarez*, 1994]. In this setup, there is no topography and the parameterization suite is replaced by a relaxation of temperature toward a zonally symmetric state and Rayleigh damping of low-level winds to emulate boundary layer friction [*Held and Suarez*, 1994]. This forcing results in a statistical mean state similar to Earth's atmosphere in terms of producing similar time-averaged zonal jet streams and temperature profiles. The only physical source/sink of AAM in this setup is the Rayleigh damping. The absence of mountain torques and other large subgrid-scale torques makes the Held-Suarez test a good test bed for investigating AAM properties of general circulation models developed for Earth's atmosphere.

The paper is organized as follows. In section 2, the formulas and associated nomenclature for the AAM analysis is introduced. The detailed global AAM analysis is presented in section 3 after a description of the exact CAM-SE dynamical core configuration in terms of polynomial order, viscosity coefficients, time steps, etc. We end the paper with a summary and discussion in section 4.

2. Method

2.1. Continuous AAM

When choosing the usual spherical coordinate system that rotates with the atmosphere and with coinciding rotation axes, the global axial angular momentum (AAM) can be separated into one part (M_r) associated with the relative motion of the atmosphere with respect to the planets surface (also known as *wind AAM*) and another part (M_Ω) associated with the angular velocity Ω ($=2\pi/d$, where d is the length of the day) of the planet (also known as *mass AAM*):

$$M = M_r + M_\Omega = \int_{\mathcal{D}} \rho u r \cos\theta \, dV + \int_{\mathcal{D}} \rho \Omega r^2 \cos^2\theta \, dV, \tag{1}$$

where r is the radial distance from the center of the planet, ρ is the fluid density, u is the zonal velocity component, θ is the latitude, λ is longitude, $dV = r^2 \cos\theta \, d\lambda \, d\theta \, dr$ is an infinitesimal spherical volume, and $\mathcal{D}$ is the global domain. We make the shallow atmosphere assumption and hydrostatic assumption so r in (1) is replaced with R (mean radius of the planet) and $dr = -\frac{1}{\rho g} dp$ (g is the gravitational constant), respectively.

In the absence of any surface torque and zonal mechanical forcing, the hydrostatic primitive equations conserve the globally integrated AAM when assuming a constant pressure upper boundary [see, e.g., *Staniforth and Wood*, 2003]:

$$\frac{dM}{dt} = 0. \tag{2}$$

Typically, numerical models are divided into a dynamical core (*dyn*) that, roughly speaking, solves the equations of motion on resolved scales and physical parameterizations that approximate subgrid-scale processes (*phys*). There can therefore be two sources/sinks of AAM:

$$\frac{dM}{dt} = \left(\frac{dM}{dt}\right)_{dyn} + \left(\frac{dM}{dt}\right)_{phys}. \tag{3}$$

In Held-Suarez configuration, $\left(\frac{dM}{dt}\right)_{phys}$ is from simplified surface drag that acts on the velocity components only. Consequently, it does not alter M_Ω but only M_r. In the Held-Suarez setup, the sources/sinks of AAM in the dynamical core are due to numerical errors unless explicit or implicit diffusion is designed to mimic physical drag. In this study, we assume that the dynamical core approximates the solution to the hydrostatic primitive equations and not any subgrid-scale processes and it should therefore, according to (2), not be a source/sink of global AAM. The spurious contributions to AAM should be much smaller than the physical sources/sinks of AAM:

$$0 \sim \left(\frac{dM}{dt}\right)_{dyn} \ll \left(\frac{dM}{dt}\right)_{phys}. \tag{4}$$

The change of total AAM due to the dynamical core, $\left(\frac{dM}{dt}\right)_{dyn}$, is decomposed into two components

$$\left(\frac{dM}{dt}\right)_{dyn} = \left(\frac{dM}{dt}\right)_{inviscid} + \left(\frac{dM}{dt}\right)_{diff}. \tag{5}$$

The first term on the right-hand side of (5) is the tendency of AAM due to "inviscid dynamics" or more precisely, dynamics without any explicit diffusion operators, which is accounted for in the second term. Explicit

diffusion in the CAM-SE model is fourth-order hyperviscosity on all prognostic variables as well as additional damping of divergent modes.

2.2. Discretization of Total AAM in CAM-SE

CAM-SE is a highly scalable dynamical core based on a equiangular cubed-sphere tiling of the sphere with elements. Within each element, the variables are represented as polynomials on a Lobatto-Legendre quadrature (GLL) grid. Hence, gradient, curl, and other operations can be computed exactly and then projected on to the basis. The operators are compatible (also called mimetic) so key discrete operators and discrete integrals satisfy continuum properties [*Taylor and Fournier*, 2010]. In particular, mass is conserved to machine precision. In the version of CAM-SE based on the *Simmons and Burridge* [1981] vertical coordinate/advection, total energy is conserved to time-truncation errors. For a detailed description of the CAM-SE dynamical core, see *Neale et al*. [2010].

In CAM-SE, the two components of total AAM are discretized as

$$M_r = \frac{R^3}{g}\sum_{i=1}^{ncol}\sum_{k=1}^{nlev}\Delta p_{ik}\, u_{ik}\cos(\theta_i)\Delta A_i, \tag{6}$$

and

$$M_\Omega = \frac{\Omega R^4}{g}\sum_{i=1}^{ncol}\sum_{k=1}^{nlev}\Delta p_{ik}\cos^2(\theta_i)\Delta A_i, \tag{7}$$

respectively, where Δp_{ik} is the pressure level thickness at the GLL point (cell) with index i ($ncol$ is the number of GLL points in each model layer) and vertical index k ($nlev = 30$ is the number of vertical levels), and ΔA_i can be interpreted as the fictitious spherical area associated with GLL point i which in CAM-SE is the product between Gauss-Legendre weights and metric terms (the weights and metric terms are so that $\sum_{i=1}^{ncol}\Delta A_i$ equals the area of the unit sphere ($=4\pi$)) [*Dennis et al*., 2012]. The terms in the AAM budget are computed "inline" in the code at every time step, i.e., $\left(\frac{dM}{dt}\right)_{dyn}$ is computed at every Runga-Kutta stage that makes up the dynamics time step ($\Delta t_{dyn}=360$s). The AAM tendencies over each Runga-Kutta stage are accumulated over each physics time step ($\Delta t_{phys}=1800$s). For the Lagrangian vertical coordinate version of CAM-SE, the vertical remapping occurs every half hour. Hence, the vertical coordinate "floats" for five dynamics time steps.

3. Results

The horizontal resolution in CAM-SE is specified through the number of elements (*ne*) and number of Gauss-Lobatto-Legendre quadrature (GLL) points along the edge of each element (*np*). With $np = 4$, the prognostic variables are represented with degree 3 ($=np-1$) polynomials in each element. Here we consider *ne*30*np*4, *ne*45*np*3, and *ne*90*np*2 configurations that all have the same number of degrees of freedom ($=6\times ne^2\times(np-1)^2$) but decreasing polynomial orders. Fourth-order viscosity is applied to all prognostic variables. The hyperviscosity coefficients for fourth-order viscosity and additional fourth-order divergence damping ($\nu=1.0\times10^{15}\mathrm{m}^4/\mathrm{s}$ and $\nu_{div}=2.5\times10^{15}\mathrm{m}^4/\mathrm{s}$, respectively), and time steps are held fixed for all *ne* and *np* settings (time steps are given in section 2.2). In the upper three levels of the model (also known as the model sponge), there is additional Laplacian damping of the prognostic variables with coefficients increasing from ν_{top},$2\times\nu_{top}$, to $4\times\nu_{top}$ toward the model top ($\nu_{top}=2.5\times10^5\mathrm{m}^2/\mathrm{s}$).

The vertical resolution is held fixed ($nlev = 30$); however, as mentioned in section 1, we consider two different vertical coordinates or equivalently two treatments of vertical advection terms in the prognostic equations referred to as "Eulerian" and "Lagrangian." The Eulerian configuration is based on finite differences that conserve energy and angular momentum [*Simmons and Burridge*, 1981]. The vertical Lagrangian coordinate configuration follows the *Lin* [2004] approach where the hybrid-sigma vertical coordinate surface are

allowed to float as material surfaces for several consecutive time steps (1800s in this study) where after the prognostic variables are remapped back to the hybrid-sigma (Eulerian) coordinate surfaces.

The default polynomial order used for (climate) simulation in CAM-SE is degree three ($np = 4$) with the above-mentioned settings for hyperviscosity operators and time steps. The preferred choice of vertical coordinate in climate simulation is the one based on floating Lagrangian levels. We will refer to this configuration as the default configuration.

The Held-Suarez forcing simulations were performed for 4000 days although we will only show results for shorter time periods after the initial spin-up. After the initial spin-up ($\sim$100 days), the global AAM diagnostics are stable; for clarity, we only show 300 day periods on the figures. As mentioned above, the AAM diagnostics were computed at every internal time step inline in the source code using native surface integration routines to integrate AAM over each element. Hence, AAM diagnostics are completely consistent in space and time with the dynamical core numerical discretization techniques. Common practice, however, is to compute AAM based on temporally averaged output of prognostic variables (six hourly or daily) and subsequent perform mathematical operations to derive AAM.

3.1. Conservation of AAM in Default Setup

Figures 2 and 3 (row 1) show the temporal evolution (day 1000–1300) of total AAM, wind AAM (M_r), and mass AAM (M_Ω) in columns 1, 2, and 3, respectively. The AAM for the default setup is shown with solid green lines (*ne*30*np*4*Lagrangian*) in Figure 2. As expected, the total AAM is dominated by the mass AAM which is about 2 orders of magnitude larger than the wind AAM. The total AAM oscillates around $\sim 1.0395 \times 10^{28}$ kg m^2/s with deviations of about 10^{25} kg m^2/s. Overall, these values are similar to real Earth AAM in terms of relative values and amplitude of the temporal variation of AAM [*Egger et al.*, 2007].

Rows 2 and 3 of Figures 2 and 3 show the relative contributions to total change in AAM due to the dynamical core, $((\frac{dM}{dt})_{dyn})$, and parameterizations, $((\frac{dM}{dt})_{phys})$, respectively, again separated into total (column 1), wind (column 2), and mass (column 3) AAM. Note that for clarity rows 2 and 3 use the same *y* axis scale (max/min values are $\pm 7 \times 10^{19}$). Since $((\frac{dM}{dt})_{dyn})$ is small a plot with a 100 times smaller range ($\pm 7 \times 10^{17}$) is embedded in the plot. We note that for the default configuration the spurious sources/sinks of total AAM are about 3 orders of magnitude smaller than the parameterized (physical) sources/sinks (equation (4)). This result is in sharp contrast to the results for CAM-FV shown in Figure 1 where the spurious sources/sinks from the dynamical core were the same order of magnitude as the parameterized sources/sinks.

In examining the breakdown of $((\frac{dM}{dt})_{dyn})$ into wind and mass tendencies for AAM (row two, columns two and three in Figures 2 and 3, respectively), it is observed that the amplitudes of these are of order 10^{19}, whereas the residual is of order 10^{16}. Hence, they balance each other to the per mil. In other words, $((\frac{dM_r}{dt})_{dyn})$ compensates very well to fluctuations in mass during advection $(\frac{dM_\Omega}{dt})$. Consequently, the fluctuations in *M* comes entirely from the parameterizations (at least up to the third digit).

By further separating $((\frac{dM}{dt})_{dyn})$ into contributions from "inviscid" dynamics, $(\frac{dM}{dt})_{inviscid}$, and hyperviscosity $(\frac{dM}{dt})_{diff}$, similar balances are observed (Figures 4 and 5). The breakdown of "inviscid" tendencies of total AAM into wind and mass AAM tendencies shows the same balance as for $((\frac{dM}{dt})_{dyn})$ in terms of magnitudes (row 2 of Figures 2 and 3 are qualitatively indistinguishable from row 1 of Figures 4 and 5; the scales on the *y* axis are identical). The diffusion (hyperviscosity) contributions to the change in AAM is dominated by velocity AAM with $(\frac{dM_r}{dt})_{inviscid}$ approximately 2 orders of magnitude larger than $(\frac{dM}{dt})_{diff}$; note that the max/min of the *y* scale of the embedded plots in Figures 4 and 5 are $\pm 1.3 \times 10^{17}$ for columns 1 and 2, whereas the range of column 3 is $[-1.2 \times 10^{15}, 0.2 \times 10^{15}]$.

In the remainder of this paper, we assess how different operator and discretization options (available in CAM-SE) affect the conservation of AAM. The impact on conservation of AAM by changing polynomial degree, change vertical coordinate and make other more subtle changes in the dynamical core, is discussed in three separate sections below.

3.2. Polynomial Order and AAM Conservation

One may readily pose the question if the AAM conservation properties are a function of the formal order of accuracy of the operators employed in the dynamical core. Since CAM-SE is based on a Galerkin method, it is rather straight forward to alter the formal accuracy of the horizontal operators by reducing the

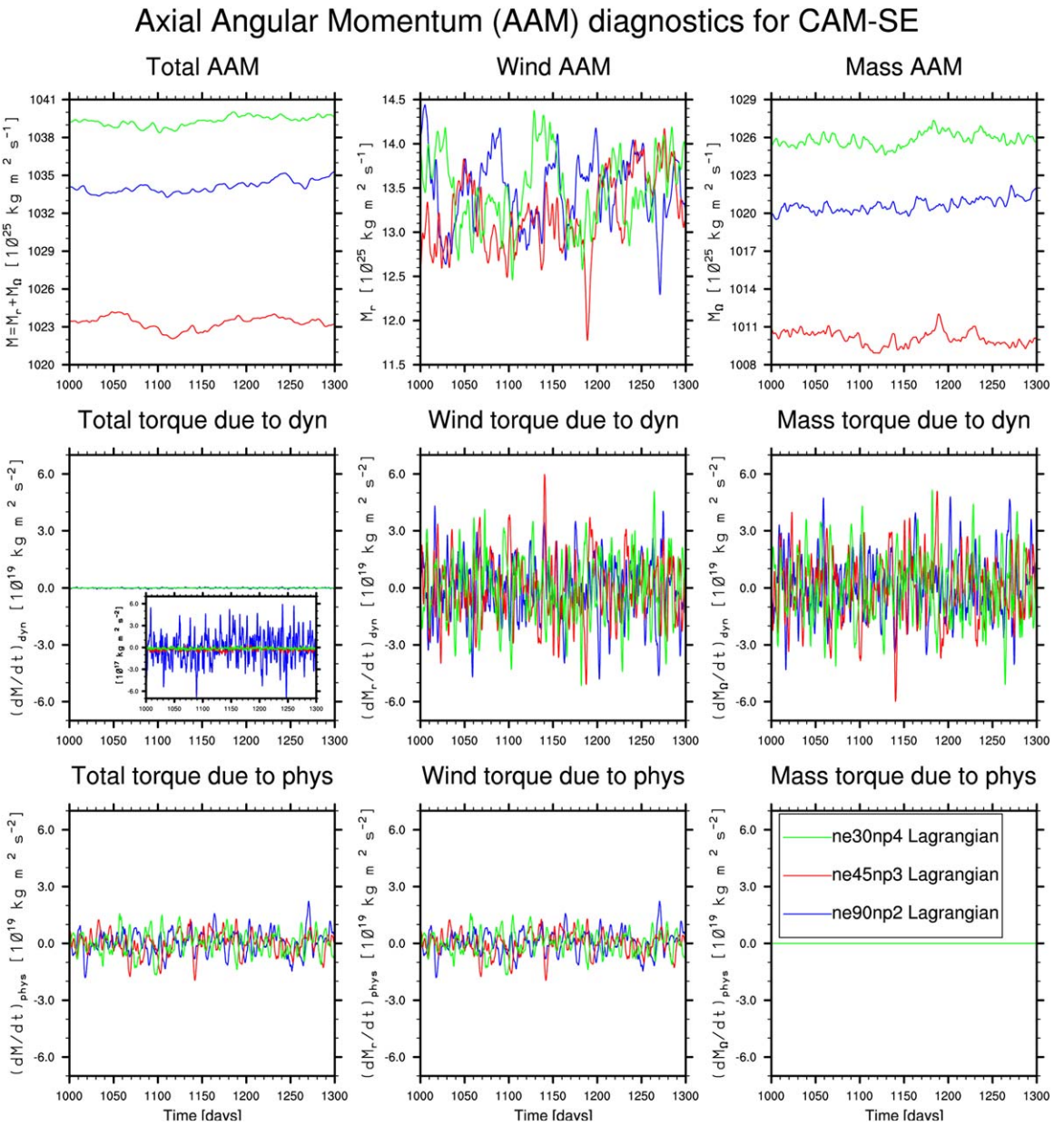

Figure 2. (row 1) Depicts (column 1) total or absolute AAM (M), (column 2) the Ω AAM (M_Ω), and (column 3) relative AAM (M_r) as a function of time (day 1000–1300) for different polynomial orders for CAM-SE based on Lagrangian vertical coordinates. Time tendencies of AAM due to the (row 2) dynamical core $\left(\left(\frac{dM}{dt}\right)_{dyn}\right)$ and (row 3) physical parameterizations $\left(\left(\frac{dM}{dt}\right)_{phys}\right)$ with the same partitioning as row 1. Note that the y axis unit on row 1 is $10^{25}\,\mathrm{kg\,m^2 s^{-1}}$, whereas the remaining rows are $1.0\times10^{19}\,\mathrm{kg\,m^2 s^{-2}}$. In the embedded plot (row 2, column 1) the unit is $1.0\times10^{17}\,\mathrm{kg\,m^2 s^{-2}}$.

polynomial order from four to three (*ne*45*np*3) and two (*ne*90*np*2). The total number of degrees of freedom held constant (number of elements is increased accordingly), i.e., the resolution for all configurations is ∼1°. All other parameters are held fixed.

Without loss of generality in this discussion we focus on Figures 2 and 4 (floating Lagrangian vertical coordinate solutions). In terms of the time evolution of total AAM, the amplitudes of the fluctuations are very similar for the fourth-order ($np = 4$; green line), third-order ($np = 3$; red line), and second-order ($np = 2$; blue line) solutions. There is an ∼5% relative difference between the time-mean values of M_r between the model configurations (Figure 4, top middle).

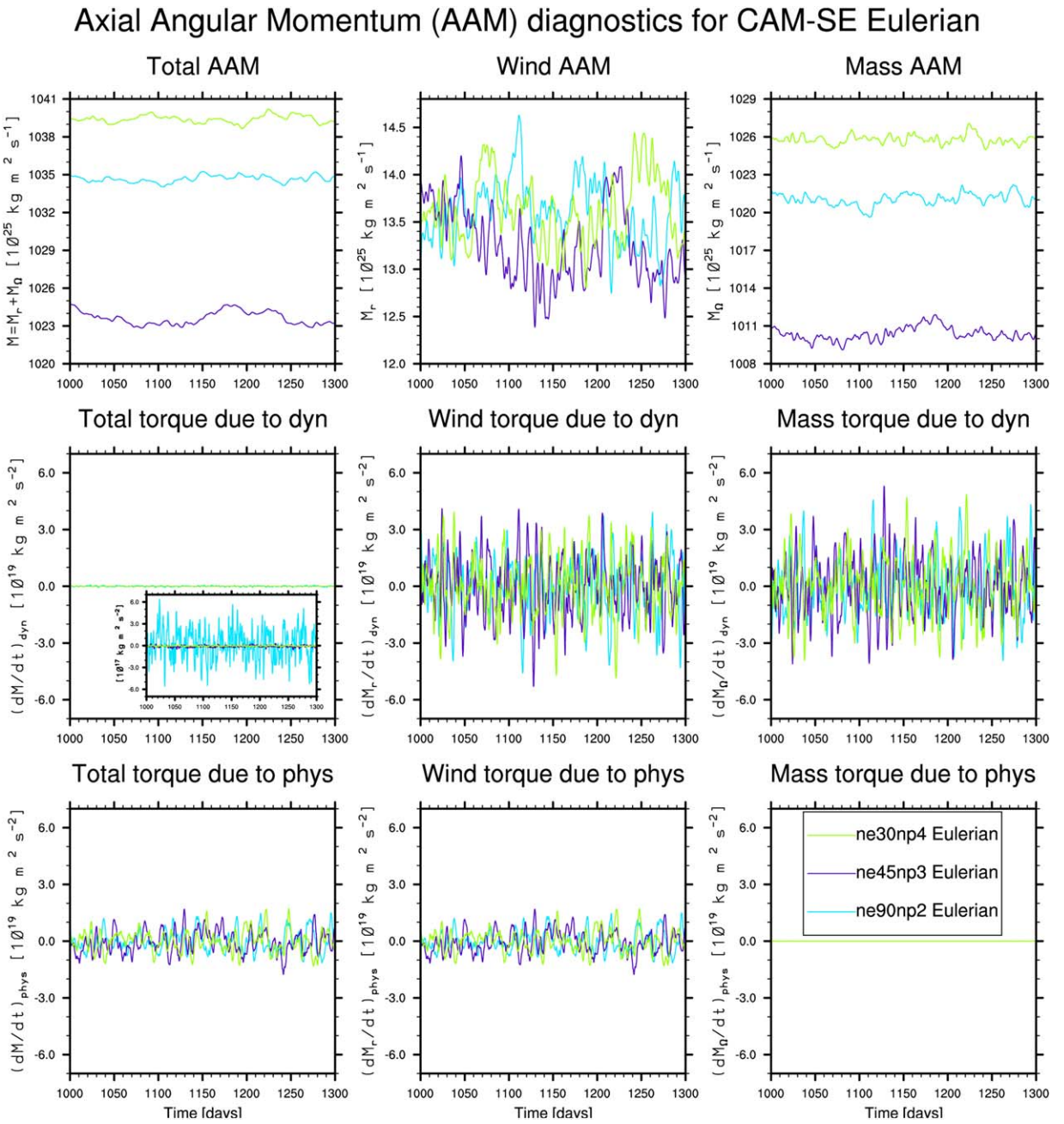

Figure 3. Same as Figure 2 but for CAM-SE based on Eulerian (hybrid-sigma) vertical coordinates.

The spurious contributions to AAM from the dynamical core is only weakly dependent on polynomial order. The second-order solution ($np = 2$) has about an order of magnitude larger contributions to AAM than the higher-order solutions. However, the spurious contributions are still 2 orders of magnitude smaller than the physical sources/sinks, i.e., the balance between wind and mass AAM is still very well maintained despite the formal low order of accuracy. As for the $np = 4$ results, the change in AAM is mainly due to "inviscid" dynamics (Figure 4).

3.3. Eulerian and Lagrangian Vertical Advection

Since both the [*Simmons and Burridge*, 1981] vertical discretization and the floating Lagrangian coordinates [*Starr*, 1945; *Lin*, 2004] are available in CAM-SE, it provides a unique opportunity to compare these vertical

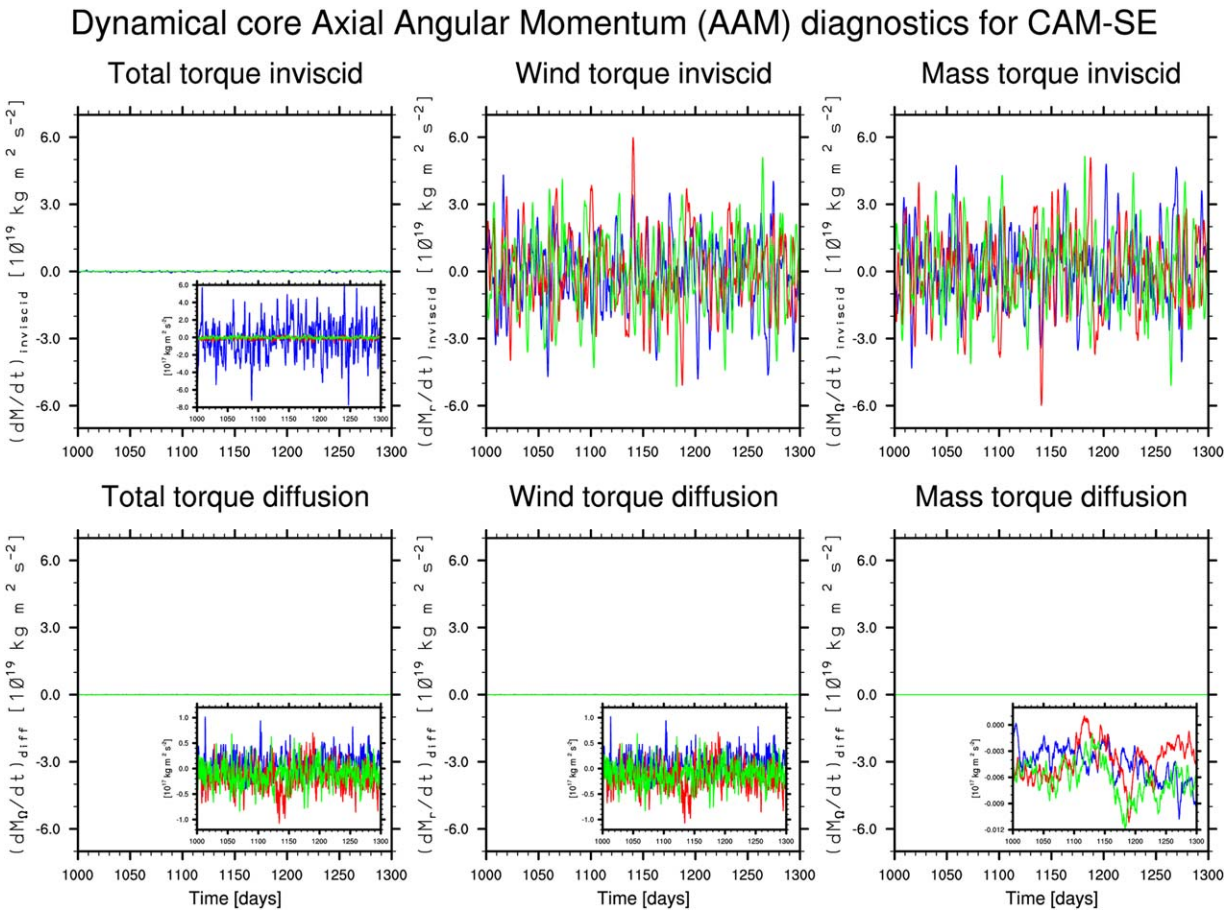

Figure 4. Same as rows 2 and 3 of Figure 2 but for the "inviscid" part of the dynamical core solver and explicit diffusion operators, respectively.

advection approaches. The simulations with different order of polynomials were repeated with the floating Eulerian (hybrid-sigma) vertical coordinate. The AAM diagnostics are plotted in Figures 3 and 5.

Both vertical advection operators conserve AAM; however, the frequency of the vertical advection step is different between the two. In the Eulerian vertical coordinate version, the vertical advection is performed at every dynamics time step. With the floating Lagrangian vertical coordinate, the vertical advection (remapping) is only performed every fifth dynamics time step.

Perhaps surprisingly we see very little dependency on vertical coordinate and AAM conservation (Figures 2–5). The main difference is on the embedded plot in Figures 4 and 5 (column 3, row 2). Since the Eulerian vertical coordinate version does not have any explicit diffusion on pressure, the mass AAM tendency $\left(\frac{dM_\Omega}{dt}\right)_{diff}$ is zero. The floating Lagrangian vertical coordinate version of CAM-SE applies explicit diffusion to pressure-level thickness and hence the mass tendencies of AAM associated with diffusion are nonzero.

3.4. Other Numerical Configuration Changes and AAM

A number of experiment were performed altering different aspects of the CAM-SE dynamical core, however, none of them changed the total AAM budget significantly (Figures 6 and 7). The experiment configurations were as follows:

1. Five-fold increase in hyperviscosity coefficient ($\nu = 5.0 \times 10^{15}$),
2. Turnoff increased divergence damping ($\nu_{div} = \nu = 1.0 \times 10^{15}$),
3. Remove uniform rotation correction in the hyperviscosity computation,
4. Change from piecewise parabolic method (PPM) [*Colella and Woodward*, 1984] vertical remapping algorithm to the piecewise spline method (PSM) [*Zerroukat et al.*, 2006],

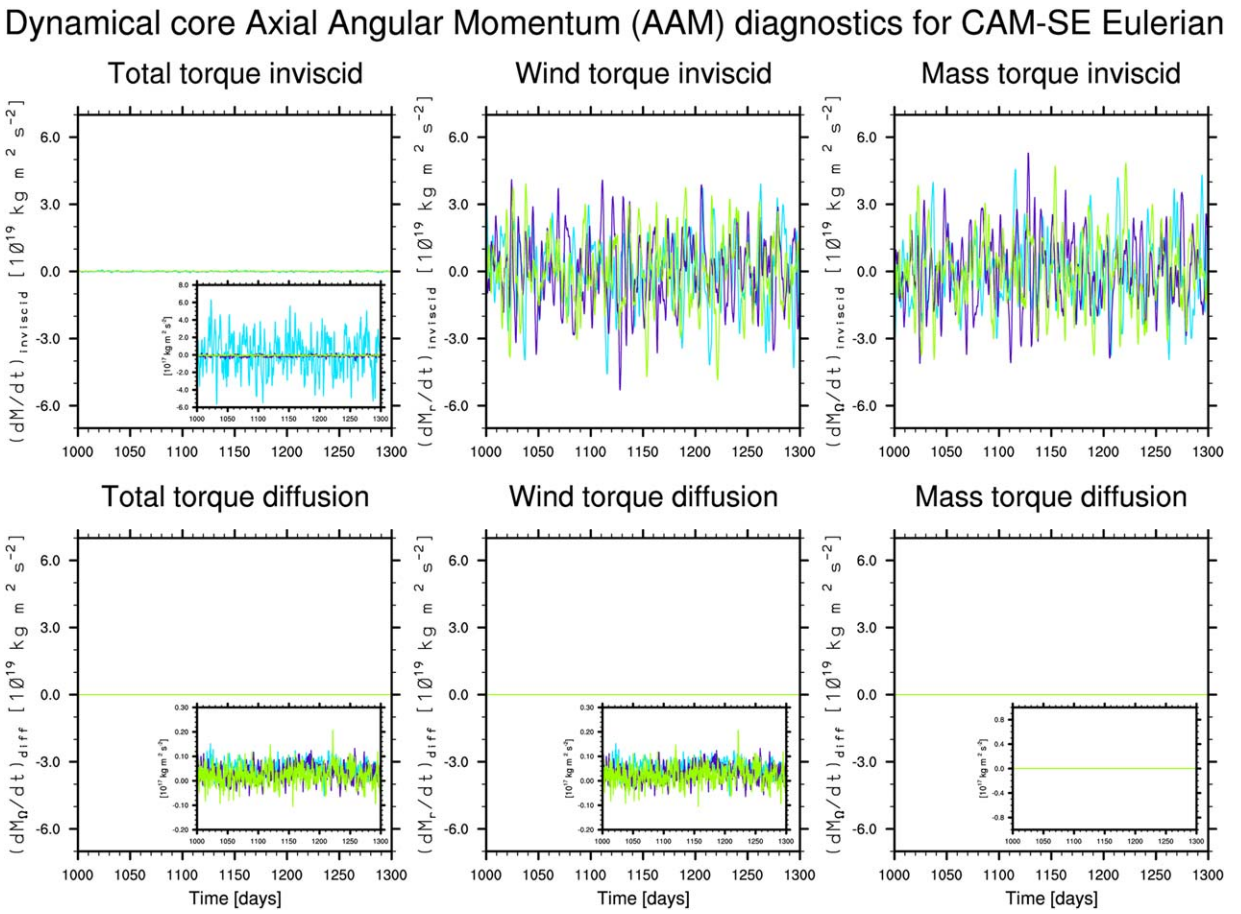

Figure 5. Same as rows 2 and 3 of Figure 3 but for the "inviscid" part of the dynamical core solver and explicit diffusion operators, respectively.

5. Turn global total energy-fixer off,
6. Turnoff sponge layer diffusion, i.e., no increase diffusion near model top (namelist variable nu_top changed from 2.5×10^5 to zero),
7. In vertical remapping algorithm (diagnostics not shown in Figures 6 and 7): instead of remapping temperature remap total energy and diagnose temperature [*Lin*, 2004].

4. Summary and Discussion

It has been shown using the Held-Suarez idealized Earth setup that NCAR's Community Atmosphere Model Spectral Element (CAM-SE) dynamical core conserves axial angular momentum very well. That said, even if good global conservation of AAM is demonstrated, it cannot be ruled out that local conservation errors somehow cancel out. Nevertheless local conservation implies global conservation, so any defects in the global conservation point to deficiencies in local conservation.

In CAM-SE, the spurious sources and sinks of AAM from the dynamical core are 3 orders of magnitude smaller than the physical (parameterized) sources/sinks. Changing the vertical coordinate from the popular *Simmons and Burridge* [1981] method to floating Lagrangian vertical coordinates [*Starr*, 1945; *Lin*, 2004] did not affect the global AAM budget. A slight degradation on the conservation of total AAM was observed when changing from formally fourth-order spatial discretization to second order, however, the spurious dynamical core sources/sinks were still 2 orders of magnitude smaller than the change in angular momentum due to physical forcing. Changing vertical remapping algorithm, increasing hyperviscosity, decreasing divergence damping, remapping total energy instead of temperature in the floating Lagrangian vertical coordinate version, turning global energy-fixer off, remove uniform rotation correction in diffusion operator

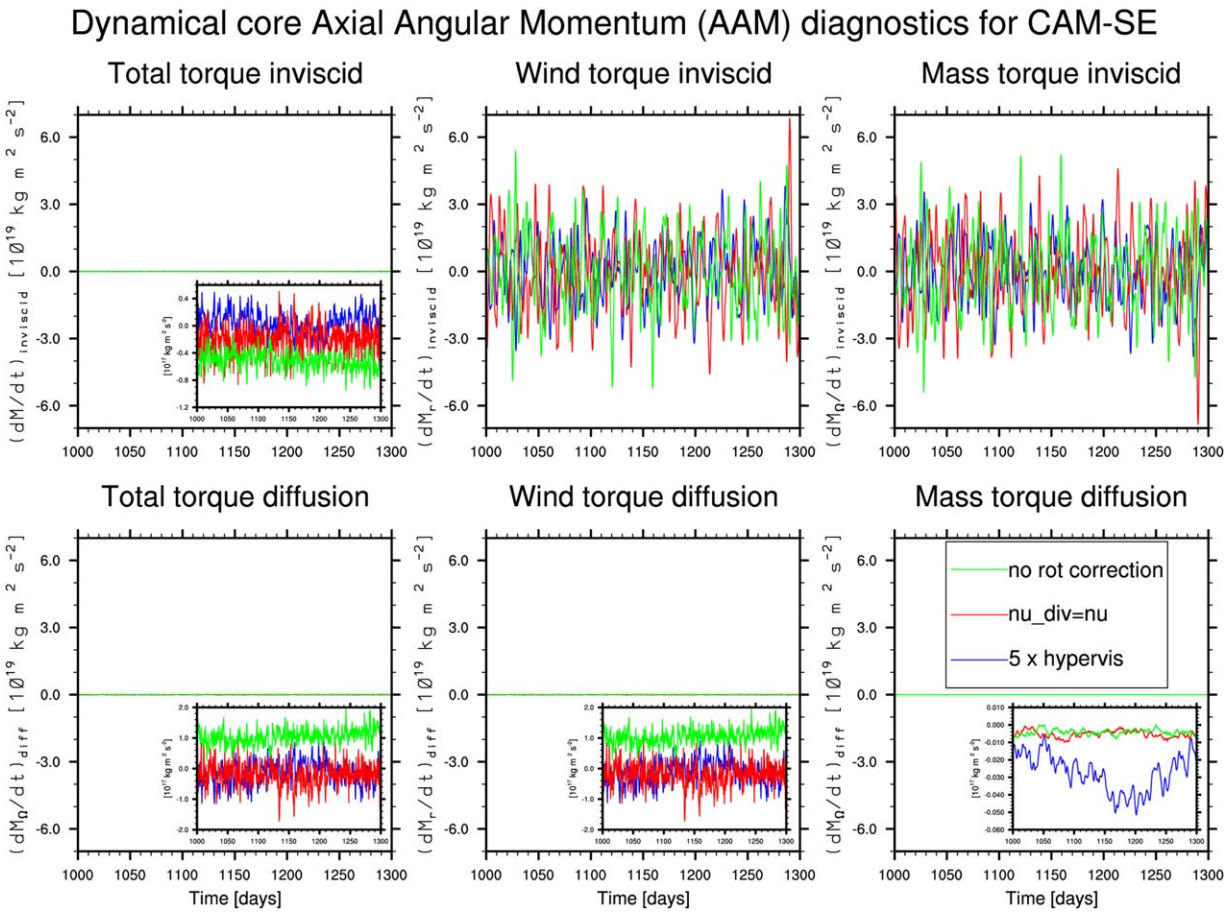

Figure 6. Same as Figure 4 but for *ne*30*np*4 based on Lagrangian vertical coordinates where different aspects of dynamical core were altered: fivefold increase in hyperviscosity coefficient ($\nu = 5.0 \times 10^{15} m^4/s$; blue line), turnoff increased divergence damping ($\nu_{div} = \nu = 1.0 \times 10^{15} m^4/2$; red line), and remove uniform rotation correction in the hyperviscosity computation (green line).

(so that uniform rotation is damped), and turning off increased sponge layer diffusion, did not significantly affect the magnitude of the spurious sources/sinks of global AAM.

In the literature, excellent AAM conservation properties have been reported in a model based on the spectral transform method [*Lee and Richardson*, 2012]. The CAM-SE and global spectral transform dynamical cores share some aspects such as colocation of prognostic variables (Arakawa *A*-grid staggering), make use of basis functions so derivative and integrals can be exactly computed (except for nonlinear terms), and the diffusion operators are higher order (typically forth order or higher). Models that have been shown (*Lee and Richardson* [2010] analyzed simplified Venus simulations with the *B*-core [*Arakawa and Lamb*, 1981], a spectral transform dynamical core [*Held and Suarez*, 1994], and a finite-volume (FV) dynamical core [*Lin*, 2004] available in the Geophysical Fluid Dynamics Laboratory (GFDL) Flexible Modeling System (FMS)) (in Venus setup) to have a larger sensitivity to "details" in the dynamical core are based finite-volume or finite difference methods [*Lee and Richardson*, 2010]. These dynamical cores are based on staggered grids and have implicit diffusion. Note that this does not necessarily imply that finite-volume and finite difference models are not suitable for simulating super-rotation. For example, the LMD GCM [*Hourdin et al*., 2006] is capable of simulating super-rotation [e.g., *Lebonnois et al*., 2010] despite being a finite difference model on a staggered grid.

That AAM conservation is, at least for CAM-SE, not primarily controlled by the vertical discretization suggests to look for the cause for good or bad conservation in the horizontal discretization. Therefore, it would be useful to analyze AAM conservation already at the level of the shallow-water equations. The simplicity of the equations may allow a more in-depth understanding of the spurious sources of AAM associated to the various discretization strategies. A first step toward such an analysis would be the specification of a shallow-

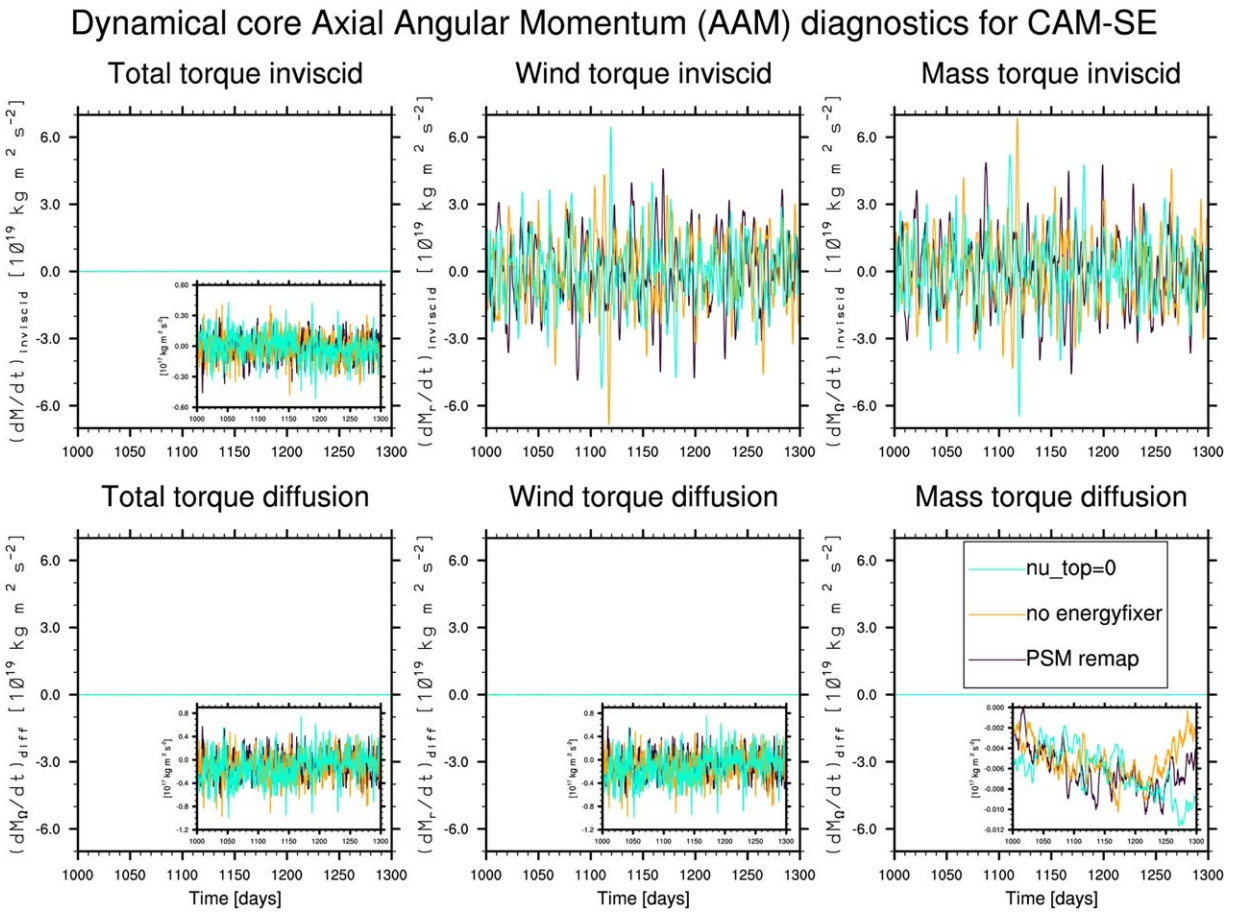

Figure 7. Same as Figure 4 but for *ne*30*np*4 based on Lagrangian vertical coordinates where different aspects of dynamical core were altered: change from piecewise parabolic method (PPM) vertical remapping algorithm to the piecewise spline method (PSM; dark gray line), turn global total energy-fixer off (orange line), and turnoff additional sponge layer diffusion (turquoise line).

water numerical experiment exacerbating defects in AAM conservation; an aspect currently overlooked by the standard test cases that numerical schemes are expected to pass [e.g., *Williamson et al*., 1992].

The authors believe that the global AAM conservation properties of CAM-SE demonstrated in this paper is an important first step in qualifying CAM-SE for the successful simulation of super-rotating atmospheres [*Parish et al*., 2012]. Contrary to the global spectral transform models widely used for Venus and Titan modeling, CAM-SE has been demonstrated to be highly scalable on massively parallel compute architectures [*Taylor et al*., 2008]. CAM-SE has also successfully been used to simulate the Quasi-Biennial Oscillation (QBO) [*Richter et al*., 2014].

Acknowledgments

The authors thank two anonymous reviewers for their reviews. NCAR is sponsored by the National Science Foundation (NSF). Partial support for this work was provided through the Scientific Discovery through Advanced Computing (SciDAC) program (DE-SC0006745) funded by U.S. Department of Energy, Office of Science, Advanced Scientific Computing Research. The discussions with J.-F. Lamarque (NCAR) and the software engineering support from B. Eaton (NCAR), S. Santos (NCAR), and S. Goldhaber (NCAR) is gratefully acknowledged.

References

Arakawa, A., and V. R. Lamb (1981), A potential enstrophy and energy conserving scheme for the shallow water equations, *Mon. Weather Rev.*, *109*, 18–36.

Colella, P., and P. R. Woodward (1984), The piecewise parabolic method (PPM) for gas-dynamical simulations, *J. Comput. Phys.*, *54*, 174–201.

Dennis, J., A. Fournier, W. F. Spotz, A. St-Cyr, M. A. Taylor, S. J. Thomas, and H. Tufo (2005), High-resolution mesh convergence properties and parallel efficiency of a spectral element atmospheric dynamical core, *Int. J. High Performance Comput. Appl.*, *19*(3), 225–235, doi: 10.1177/1094342005056108.

Dennis, J. M., J. Edwards, K. J. Evans, O. Guba, P. H. Lauritzen, A. A. Mirin, A. St-Cyr, M. A. Taylor, and P. H. Worley (2012), CAM-SE: A scalable spectral element dynamical core for the Community Atmosphere Model, *Int. J. High Performance Comput. Appl.*, *26*(1), 74–89, doi: 10.1177/1094342011428142.

Egger, J., K. Weickmann, and K.-P. Hoinka (2007), Angular momentum in the global atmospheric circulation, *Rev. Geophys.*, *45*, RG4007, doi: 10.1029/2006RG000213.

Held, I. M., and M. J. Suarez (1994), A proposal for the intercomparison of the dynamical cores of atmospheric general circulation models, *Bull. Am. Meteorol. Soc.*, *75*, 1825–1830.

Hourdin, F. (1992), Conservation du moment cinétique dans le modèle de circulation générale du LMD, *Tech. Rep. 175*, Lab. de Météorol. Dyn., Paris. [Available at http://lmdz.lmd.jussieu.fr/developpeurs/notes-techniques/ressources/conserv.pdf.].

Hourdin, F., et al. (2006), The LMDZ4 general circulation model: Climate performance and sensitivity to parameterized physics with emphasis on tropical convection, *Clim. Dyn.*, *27*(7–8), 787–813, doi:10.1007/s00382-006-0158-0.

Lebonnois, S., F. Hourdin, V. Eymet, A. Crespin, R. Fournier, and F. Forget (2010), Superrotation of venus' atmosphere analysed with a full general circulation model, *J. Geophys. Res.*, *115*, E06006, doi:10.1029/2009JE003458.

Lebonnois, S., C. Covey, A. Grossman, H. Parish, G. Schubert, R. Walterscheid, P. H. Lauritzen, and C. Jablonowski (2012), Angular momentum budget in general circulation models of superrotating atmospheres: A critical diagnostic, *J. Geophys. Res.*, *117*, E12004, doi:10.1029/2012JE004223.

Lee, C., and M. Richardson (2012), Angular momentum conservation in a simplified venus general circulation model, *Icarus*, *221*(2), 1173–1176, doi:10.1016/j.icarus.2012.10.007.

Lee, C., and M. I. Richardson (2010), A general circulation model ensemble study of the atmospheric circulation of Venus, *J. Geophys. Res.*, *115*, E04002, doi:10.1029/2009JE003490.

Lin, S.-J. (2004), A "vertically Lagrangian" finite-volume dynamical core for global models, *Mon. Weather Rev.*, *132*, 2293–2307.

Neale, R. B., et al. (2010), Description of the NCAR Community Atmosphere Model (CAM 5.0), NCAR Technical Note NCAR/TN-486+STR, *Natl. Cent. of Atmos. Res*, Boulder, Colo.

Parish, H., S. Lebonnois, G. Schubert, C. Covey, R. Walterscheid, and A. Grossman (2012), Importance of the angular momentum budget in Venus atmosphere general circulation models, poster presented at Conference on Comparative Climatology of Terrestrial Planets, Boulder, Colo., 25–28 Jun. Available at: http://www.lpi.usra.edu/meetings/climatology2012/pdf/8017.pdf.

Richter, J. H., A. Solomon, and J. T. Bacmeister (2014), On the simulation of the Quasi-Biennial Oscillation in the Community Atmosphere Model, Version 5, *J. Geophys. Res.*, in press.

Simmons, A. J., and D. M. Burridge (1981), An energy and angular-momentum conserving vertical finite-difference scheme and hybrid vertical coordinates, *Mon. Weather. Rev.*, *109*(4), 758–766.

Staniforth, A., and N. Wood (2003), The deep-atmosphere Euler equations in a generalized vertical coordinate, *Mon. Weather Rev.*, *131*, 1931–1938, doi:10.1175//2564.1.

Starr, V. P. (1945), A quasi-Lagrangian system of hydrodynamical equations, *J. Meteorol.*, *2*, 227–237.

Taylor, M., J. Edwards, and A. St-Cyr (2008), Petascale atmospheric models for the community climate system model: New developments and evaluation of scalable dynamical cores, *J. Phys. Conf. Ser.*, *125*, 012023, doi:10.1088/1742–6596/125/1/012023.

Taylor, M. A., and A. Fournier (2010), A compatible and conservative spectral element method on unstructured grids, *J. Comput. Phys.*, *229*(17), 5879–5895, doi:10.1016/j.jcp.2010.04.008.

Thuburn, J. (2008), Some conservation issues for the dynamical cores of NWP and climate models, *J. Comput. Phys.*, *227*, 3715–3730.

Williamson, D. L., J. B. Drake, J. J. Hack, R. Jakob, and P. N. Swarztrauber (1992), A standard test set for numerical approximations to the shallow water equations in spherical geometry, *J. Comput. Phys.*, *102*, 211–224.

Zerroukat, M., N. Wood, and A. Staniforth (2006), The parabolic spline method (PSM) for conservative transport problems, *Int. J. Numer. Methods Fluids*, *51*, 1297–1318.